

The Utility of X-Radiography for Generation of High-Resolution Paleoclimatic Proxy Records from Black Shales, with Examples from Core Shale Members of Upper Pennsylvanian Midcontinent Cyclothems

Thomas J. Algeo¹, David L. Hoffman^{1,*},
J. Barry Maynard¹, Michael M. Joachimski²,
James C. Hower^{3,4}, and W. Lynn Watney⁵

¹ H. N. Fisk Laboratory of Sedimentology
Department of Geology
University of Cincinnati
Cincinnati, OH 45221-0013

* Present address:
Burns & McDonnell
165 EAB Plaza, 6W
Uniondale, NY 11556-0165

² Institut für Geologie
Schlossgarten 5
University of Erlangen-Nürnberg
91054 Erlangen, Germany

³ Center for Applied Energy Research
3572 Iron Works Pike
Lexington, KY 40511-8433

⁴ Department of Geological Sciences
University of Kentucky
Lexington, KY 40506-0059

⁵ Kansas Geological Survey
1930 Constant Avenue
Lawrence, KS 66047-3724

(In: Algeo, T.J., and Maynard, J.B. (Eds.), 1997. *Cyclic Sedimentation of Appalachian Devonian and Midcontinent Pennsylvanian Black Shales: Analysis of Ancient Anoxic Marine Systems—A Combined Core and Field Workshop: Joint Meeting of Eastern Section AAPG and The Society for Organic Petrography (TSOP)*, Lexington, Kentucky, Sept. 27-28, 1997, p. 78-102.)

ABSTRACT

Ancient black shales have considerable potential for generation of long, high-resolution paleoclimate proxy records, given the availability of a geochemical proxy that can be easily measured. Owing to substantial differences in density between the siliciclastic matrix of black shales (2.6-2.7 g cm⁻³) and the major non-clastic components, i.e., organic carbon, Fe-sulfide, and phosphate (ca. 1.0-1.2, 5.1-5.2, and 3.1-3.2 g cm⁻³, respectively), rock density may represent a suitable proxy. This paper presents a new procedure for rapid analysis of fine-scale compositional variation in black shales, using X-radiography as a primary tool for measurement of rock density. The procedure entails (1) generation of X-radiographs over the complete stratigraphic interval of interest in laminated black shale cores, (2) geochemical and petrographic analysis of limited intervals within the cores to quantify variance in major rock components, and (3) statistical analysis of compositional controls on variance in X-radiograph gray-scale density (a proxy for rock density). This procedure was applied to eight study units from three offshore black shales (Hushpuckney, Stark, and Muncie Creek) of Upper Pennsylvanian cyclothems of midcontinent North America.

Multiple regression analysis revealed that three rock components (organic carbon, Fe-sulfides, and phosphate, as proxied by TC, TS, and P₂O₅ concentrations, respectively) collectively accounted for the majority of gray-scale density variance in each shale: 71% in the Hushpuckney, 87% in the Stark, and 92% in the Muncie Creek. Linear regression analysis of gray-scale density values versus concentrations of elemental proxies for the major non-clastic rock components yielded significant correlations ($p(\alpha) < .05$) between gray-scale density and (1) total carbon in seven of eight study cores ($r = -0.61$ to -0.97), (2) total sulfur in a single core (Heilman Stark; $r = +0.61$), and (3) phosphorus in a single core (Mitchellson Hushpuckney; $r = +0.87$). Consequently, gray-scale density values can be used to rapidly quantify variation in the relevant rock components at a fine (i.e., cm) scale over long stratigraphic intervals in these cores. X-radiography has considerable underexploited potential for generation of high-resolution paleoclimate proxy records and for analysis of environmental conditions during deposition of laminated organic-rich sediments.

INTRODUCTION

Analysis of secular paleoclimatic variation is facilitated by generation of stratigraphic records of sufficient temporal resolution to permit identification of high-frequency climatic signals and of sufficient length to allow analysis of climate stability and low-frequency components of variation. Ancient black shales have considerable potential for generation of long, high-resolution paleoclimate proxy records because (1) primary laminae are preserved at a fine (commonly sub-mm) scale, yielding information regarding high-frequency changes in environmental conditions (e.g., Hay et al. 1990; Lyons 1991; Peterson et al. 1991; Ripepe et al. 1991; Aplin et al. 1992; Repeta 1993), and (2) many shales are tens to hundreds of meters in thickness and represent quasi-continuous records of sedimentation over intervals of hundreds of thousands to millions of years (e.g., Potter et al. 1982). High-resolution paleoclimate proxy records of this type are useful in addressing such problems as, e.g., forcing mechanisms responsible for sedimentary cyclicity, controls on the accumulation of sedimentary organic matter, and time constraints within poorly-dated stratigraphic units.

Chemostratigraphic methods have been widely employed for generation of paleoclimate proxy records in fine-grained, deep-water stratigraphic successions, commonly in combination with a uniform sampling strategy. However, owing to the labor-intensive nature of geochemical procedures, this approach necessitates trade-offs between the length of the succession analyzed, sampling density, and the number of analytical techniques applied. Long high-density chemostratigraphic records are rarely generated for more than a single geochemical parameter, e.g., calcium carbonate content (Herbert and Fischer 1986; Sageman et al. 1997), and application of multiple geochemical techniques necessitates either a limited stratigraphic range of analysis (Wenger and Baker 1986; Desborough et al. 1991; Hatch and Leventhal 1992) or wide sample spacing (Coveney 1985; Coveney et al. 1987; Schultz and Coveney 1992). Each choice has drawbacks: (1) analysis of a single geochemical parameter may provide insufficient data to determine relations among major rock components (i.e., organics, sulfides, and clastics), (2) a limited stratigraphic range of analysis may fail to identify significant patterns of environmental variation at longer timescales or over broader areas, and (3) wide sample spacing runs the risk of overlooking high-frequency variation or of recognizing spurious signals at the limit of resolution of the data (i.e., "aliasing" in time-series parlance).

An alternative approach to generation of high-resolution paleoclimatic proxy records is to utilize a geochemical proxy that can be rapidly measured at a fine scale over long stratigraphic intervals and to establish the relationship of the proxy to underlying compositional controls through a limited

program of sampling and geochemical analysis. A method applied to porous, unlithified marine sediments is gamma-ray attenuation porosity evaluator (GRAPE) analysis, which measures saturated bulk density with a spatial resolution of 0.5-3.0 cm (Herbert and Mayer 1991; Mayer et al. 1993). Methods used on consolidated strata in outcrop or core are commonly based on measurement of optical color variation, e.g., microdensitometry (Herbert and Fischer 1986) and photographic image analysis (Sageman et al. 1997). Because these methods depend on the presence of strong color variation, they work best in marly successions exhibiting substantial variation in carbonate content. Application of these methods to black shales is precluded by a lack of sufficient color variation.

Thus, the fundamental impediment to generation of long, high-resolution paleoclimatic proxy records in black shale successions is lack of a suitable geochemical proxy that can be easily measured. In this paper, we present a new procedure for rapid analysis of fine-scale compositional variation in black shales over long stratigraphic intervals, using variation in rock density as a geochemical proxy. The method, for which X-radiography serves as the primary tool, entails (1) generation of X-radiographs over the complete stratigraphic interval of interest in laminated shale cores, providing a high-resolution record of variation in rock density (Algeo et al. 1994), and (2) geochemical and petrographic analysis of limited stratigraphic intervals, permitting identification of compositional controls on rock density (Hoffman et al. 1997; Jaminski et al. 1997). The use of X-radiography as a primary tool in compositional analysis of laminated organic-rich sediments has a number of advantages over a purely chemostratigraphic approach: (1) superior spatial resolution (i.e., sub-mm scale), (2) optimization of sampling sites for geochemical analysis through "previewing" of patterns of compositional variation, and (3) easy conversion into digital data series amenable to spectral analysis. The primary goals of this contribution are to demonstrate (1) the utility of X-radiography for generation of high-resolution geochemical proxy records, and (2) appropriate statistical procedures for determination of compositional controls on rock-density variation in laminated organic-rich sediments.

STUDY UNITS

The examples illustrated in this contribution are drawn from offshore (core) black shale members of cyclothems from the Missourian Stage (lower Upper Pennsylvanian) of Midcontinent North America (Watney 1980; Watney et al. 1989). Missourian Stage cyclothems consist of 10-50-m-thick marine limestone-shale successions deposited as transgressive-regressive cycles in response to quasi-periodic glacio-eustatic fluctuations (Crowell 1978; Veevers and Powell 1987; Heckel 1994). Core (or offshore) black shales are deepwater, condensed facies, representing maximum flooding surfaces in a sequence stratigraphic context (Heckel 1977 1984; Watney et al. 1995). In the study area, these shales are thin (40-60 cm), laminated, and non-fossiliferous, and are inferred to have been deposited under sediment-starved conditions in a distal offshore setting within a stratified anoxic marine basin (Heckel 1977, 1991; Coveney and Shaffer 1988). Slow sedimentation rates (e.g., a few mm 10^3 yr⁻¹) are inferred on the basis of fine grain size, abundance of authigenic phosphate, absence of biota other than rare pelagic or epipelagic marine organisms, and depletion of Fe-sulfides in ³⁴S, but absolute sediment accumulation rates are uncertain (Coveney et al. 1989; Watney et al. 1995). This report will examine three core black shales of the Kansas City Group (Missourian Stage) from eastern Kansas: (1) the Hushpuckney Shale Member of the Swope Formation, (2) the Stark Shale Member of the Dennis Formation, and (3) the Muncie Creek Shale Member of the Iola Formation.

METHODS

Analytical Strategy

Efficient analysis of fine-scale compositional variation in black shales over long stratigraphic intervals is possible by combining whole-core X-radiography with petrographic and geochemical analysis of selected stratigraphic intervals. The procedure entails (1) X-radiography of the complete stratigraphic interval of interest, (2) generation of gray-scale density (GSD) records from X-radiograph negatives, providing a continuous high-resolution record of rock-density variation (Algeo and Woods 1994), (3) geochemical and petrographic analysis of selected stratigraphic intervals for characterization of fine-scale compositional variation (Hoffman et al. 1997; Jaminski et al. 1997), (4) statistical analysis of compositional controls on rock-density variation, e.g., through GSD-elemental correlations, and (5) construction of proxy geochemical records based on significant GSD-elemental correlations (Fig. 1). The first two steps of the procedure, X-radiography and generation of GSD records, are discussed in detail under Methods:X-radiography below.

The goal of the third step of the procedure, geochemical and petrographic analysis of selected stratigraphic intervals, is to determine compositional controls on GSD variation. Analysis of compositional controls on rock-density variation is best undertaken at a fine (i.e., cm) scale, because (1) stronger correlations between geochemical and rock-density parameters emerge at a fine than at a coarse scale, and (2) patterns of covariation between rock parameters may change at different stratigraphic scales (e.g., large-scale positive and fine-scale negative covariation between TOC and TS; cf. Robl et al. 1983; Jaminski et al. 1997). For this reason, 1-cm-thick samples were collected contiguously over a 12-16-cm-thick stratigraphic interval corresponding to at least one complete compositional cycle in each study unit (see Methods:Sampling below). A total of eight study units were investigated (three Hushpuckney, four Stark, and one Muncie Creek core), and the overall sampling strategy was hierarchical in design to allow investigation of large-scale patterns of compositional variation in the units of interest (see description in companion paper).

The final steps of the procedure, statistical analysis of compositional controls on rock-density variation and construction of proxy geochemical records (Fig. 1), were facilitated by two conditions: (1) differences in density between the major non-clastic components and the shale matrix, and (2) availability of reliable elemental proxies for the major components. In the study units, the major non-clastic components, i.e., organic carbon, Fe-sulfide, and phosphate, differ substantially in density from that of the shale matrix (see Methods:X-radiography below). Further, these components can be proxied by TC, TS, and P_2O_5 , respectively (see Results:Elemental Proxies for Major Components below). Consequently, correlations between rock density (as proxied by X-radiograph gray-scale density) and the abundances of major components that influence rock density (as proxied by elemental parameters) can be established. Subsequent analysis entailed (1) demonstration through multiple regression analysis of significant control of GSD values in a given study unit by TC, TS, and P_2O_5 concentrations, and (2) for those components exerting a significant influence on GSD values, linear regression analysis of GSD-elemental relations, yielding an equation with predictive value for estimation of component abundances in un-analyzed portions of the study unit (see Results:GSD-Elemental Correlations below).

X-radiography

Contrast in X-radiographs is a function of the distribution of major components of differing density. For a sample of uniform thickness, denser (less dense) areas of the sample appear lighter (darker) owing to reduced (increased) X-ray penetration (e.g., Algeo and Woods 1994; Algeo et al. 1994; Jaminski et al. 1997). On the basis of petrographic and geochemical analyses, the major non-clastic components of the study units were determined to be organic carbon ($1.0\text{-}1.2\text{ g cm}^{-3}$), Fe-sulfides (mainly pyrite; $5.1\text{-}5.2\text{ g cm}^{-3}$), and phosphate ($3.1\text{-}3.2\text{ g cm}^{-3}$), each of which differs substantially in density from that of the shale matrix ($2.6\text{-}2.7\text{ g cm}^{-3}$), which is composed largely of illite, mixed-layer illite/smectite, and other clay minerals (Hoffman et al. 1997). Thus, X-radiographic contrast in the study units is mainly due to variation in the proportions of these major components (Fig. 2).

Conventional X-radiographic procedures entail cutting samples into thin slabs (commonly <10 mm thick) to minimize interference between sedimentary components and to maximize resolution in the resulting images (e.g., McKinsey and Kepferle 1985). However, sample slabbing is a time-consuming and fundamentally destructive process and is unnecessary in sedimentary rock cores containing penetrative laminae. This is because high-resolution images can be obtained from moderately thick samples (e.g., 10-50 mm) provided that the X-ray beam is collimated and held parallel to sample stratification. In horizontally laminated cores, sedimentary laminae are easily aligned with the X-ray beam through use of a lead-shielded core stage (Algeo et al. 1994). This approach has several advantages over conventional X-radiographic procedures: (1) higher and more uniform spatial resolution of images, (2) equal exposure of all parts of a sample or core interval, (3) rapidity of analysis (ca. 30 cm hr^{-1}), and (4) non-destructiveness of cores.

For this study, X-radiograph images were produced at the University of Cincinnati using a tungsten-source Hewlett Packard Faxitron (model 43804N) and a custom-built core stage consisting of a platform driven by a variable-speed step motor. Cores were X-rayed in 25-cm-long segments, and each segment was placed on the stage on top of a film holder (containing Kodak Type M film) and covered by a lead shield with a central window of adjustable width. At a source voltage of 60-70 kV, about 5 minutes of exposure was required for good image contrast, which was achieved by using a 2.5-cm-wide window and a stage speed of 0.5 cm min^{-1} . After development, X-radiograph negatives were scanned at 300-dpi resolution using a UMAC UC630 color scanner and downloaded to an Optimas image analysis system. In the image analysis system, three parallel line luminance transects were taken, i.e., along the center of the long axis of each core segment and 5 mm to either side of the center, and these were averaged to minimize the effects of fine-scale lateral compositional variation in the study units. This yielded a continuous record of variation in the gray-scale density (GSD) of the core images on a brightness scale ranging from 0 (black) to 255 (white) at a sampling density of 5.3 observations per millimeter (Fig. 2; n.b., sampling density comparable to that achieved using microdensitometry; Herbert and Fischer 1986). Consistency of results between cores was verified by inclusion of a GSD standard (i.e., a billet with well-defined GSD maxima and minima) in each negative; care was taken to follow uniform procedures, yielding consistent and reproducible results.

Sampling Procedure

In each study unit, a 12-16-cm-thick stratigraphic interval corresponding to at least one complete compositional cycle was chosen for detailed geochemical and petrographic analysis (e.g., Fig. 2). The lower to middle portion of the black shale facies (i.e., ca. 5-25 cm above base of section) was favored for this purpose owing to the presence of well-defined dm-scale compositional cyclicity and to the ease of correlation between study locales in each shale member. Each stratigraphic interval for detailed analysis was subdivided into 9-14 sample zones of subequal thickness (0.6-2.0 cm; mean 1.2 cm), yielding a total of 85 samples from the eight study units (Hoffman et al. 1997). Contacts between sample zones were picked on the basis of core X-radiographs so that the boundaries coincided with natural compositional breaks (Fig. 2). The same sample zones were used for all analytical procedures to maintain maximum intercomparability of results. Samples were ground in an agate ball mill and stored in nitrogen-filled vials and refrigerated to prevent oxidation of organic carbon and sulfides prior to analysis.

Petrographic and Geochemical Analyses

Petrographic components were examined in polished slabs under reflected white and violet-UV fluorescent light, and organic macerals were classified using standard nomenclature (Hutton 1987; Tyson 1995). Carbon and sulfur elemental concentrations of samples ($n = 85$) were determined using a LECO CS-244 analyzer. A representative subset of samples ($n = 17$), including material from each study formation and locale, was analysed for inorganic C content using a carbonate bomb. For carbon isotopic analysis of bulk organic matter, samples ($n = 61$) were treated with hot concentrated HCl to remove carbonates, washed with deionized water, combusted with CuO at 850°C in quartz tubes, and measured using a Finnegan MAT 252 mass spectrometer. Major-, minor-, and trace-element concentrations ($n = 85$) were determined using a wavelength-dispersive Rigaku 3040 XRF spectrometer, and the mineralogic composition of a small number of whole-rock and clay-mineral separates ($n = 10$) was determined using a Siemens X-ray diffractometer. Leco analysis was undertaken at the Kentucky Geological Survey, C-isotopic analysis at the University of Erlangen-Nürnberg, Germany, and all other procedures at the University of Cincinnati. See the companion paper for a full description of methods, including instrumental precision and detection limits.

RESULTS

Core X-radiography

Patterns of fine-scale compositional variation in the study units were initially identified using X-radiographs, which permitted detailed observations regarding compositional layering and the distribution of authigenic precipitates. The black shale facies of all study units is characterized by compositional layering at two scales: (1) faint, horizontal, sub-mm-thick laminae, and (2) dm-scale light-dark banding. The dm-scale couplets (which range from about 5 to 15 cm in thickness) are weakly visible on core surfaces as alternating dark gray (Munsell 10 YR 6/1-5/1) and black layers (Munsell 10 YR 3/1-2/1) but are strongly enhanced in X-radiographs (Fig. 2), which measure rock-density rather than optical color variation. The primary control on dm-scale variation in rock density is organic carbon content (see Results:GSD-Elemental Correlations below), which varies from 10-20 wt% TOC in the comparatively organic-poor light bands (darker in prints) to 20-40 wt% TOC in the organic-rich dark bands (lighter in prints; e.g., Fig. 2).

In addition to compositional layering, X-radiographs provided information about the distribution of authigenic phases. Phosphate and Fe-sulfides are components of higher density than the shale matrix and, hence, result in darker X-radiograph images. Phosphate has a distinctive morphology, e.g., smooth ovoid nodules, small granules, and wispy laminae, and occurs mainly as macroscopic features with sharply-defined contacts, facilitating visual identification in core X-radiographs (e.g., Fig. 2). Individual phosphatic layers are thin (<1 cm, and commonly <1 mm), and most layers are laterally discontinuous at a centimeter scale. For the most part, phosphate layers occur in sets that are several centimeters in thickness; nodule character tends to be similar within each set but to differ between sets. Authigenic phosphate appears to be concentrated mainly at the upper and lower contacts of high-TOC layers and, hence, may have been released from organic matter and reprecipitated at redox boundaries within the sediment column (e.g., Jarvis et al. 1994). Fe-sulfides occur as microscopic grains that are finely disseminated throughout the shale matrix, making their distribution impossible to ascertain from visual inspection of X-radiographs.

Elemental Proxies for Major Components

In order to utilize X-radiograph gray-scale density (GSD) for compositional analysis, it is necessary to correlate GSD values with the abundances of major non-clastic components. The most direct means of quantifying component abundances is to identify an elemental proxy for each component. In the study units, organic carbon, Fe-sulfides, and phosphate can be proxied by TC, TS, and P₂O₅, respectively. Total organic carbon (TOC) is effectively proxied by total carbon (TC), because total inorganic carbon (TIC) makes up an insignificant fraction of rock mass (mean 0.2±0.2 wt%) and TC (mean 0.9±0.9%; ±1σ; n = 17; Fig. 3). TOC, which was determined by difference, thus represents 99.1±0.9% of TC on average. The uniformly low concentration of TIC was verified by (1) point-counts yielding <1 vol% CaCO₃ in all samples, and (2) lack of evolution of CO₂ upon random acid checks of the cores. The full sample set (n = 85) yielded a mean TC value of 18.7±8.2 wt% (±1σ). Organic matter in offshore shales of eastern Kansas is of relatively low maturation rank (Wenger and Baker 1986), and thermal alteration or destruction of organic constituents in the burial environment is not a major concern.

Fe-sulfide content may be proxied by total sulfur (TS), although some fraction of TS represents organic sulfur (commonly ca. 10-20%; e.g., Robl et al. 1983) and phosphate sulfur (probably no more than a few percent). Total sulfur averages 2.13±0.69 wt% (±1σ) in the study units, which is equivalent to a volumetric concentration of 1.8±0.6%, if 100% of TS is assumed to reside in pyrite. Actual petrographic estimates of mean pyrite abundance (8±8 vol%) are probably too high but serve to verify the presence of a substantial Fe-sulfide component in the study units. Fe-S relations also provide constraints on the distribution of sulfur among major rock components. Strong positive covariation between S and Fe in some study units (e.g., Edmonds and Ermal Stark shales; Fig. 4) suggests that a large proportion of sulfur resides in Fe-sulfides and that iron is highly sulfidized (i.e., largely sequestered in pyrite). TC-TS relations are consistent with this inference: most samples fall well below the "normal" marine trend for oxic-suboxic environments (Berner and Raiswell 1983), are poorly correlated ($r^2 = 0.10-0.46$), and exhibit positive regression Y-intercepts (1.0-1.8 wt% TS), indicating Fe-limited conditions of pyrite formation (Hoffman et al. 1997). Determination of pyrite sulfur concentration by chromium reduction analysis (Canfield et al. 1986) is in progress and will provide further constraints on the distribution of sulfur among major components of the study units.

Phosphate is effectively proxied by P₂O₅ in the study units because almost all P is concentrated

in authigenic phosphate nodules (Hoffman et al. 1997). This relation is demonstrated by strong covariance between P_2O_5 and CaO in the study units ($r^2 = 0.95$; Fig. 5). Total phosphorus averages 3.05 ± 3.66 wt% ($\pm 1\sigma$) in the study units. All samples containing macroscopic phosphate nodules exhibited significant P_2O_5 enrichment (>5 wt%), whereas those lacking visible phosphate nodules yielded uniformly low P_2O_5 values (<0.5 wt%; Hoffman et al. 1997). As a consequence, areas of high-P versus low-P content in the study cores are easily identified through visual inspection of core X-radiographs, in which most discrete, dark (i.e., dense) features represent authigenic phosphate nodules (Fig. 2). Although Fe-sulfides are dense enough to mimic phosphate nodules, pyrite is generally finely disseminated through the shale matrix and macroscopic occurrences are rare.

GSD-Elemental Correlations

Once elemental proxies for the major non-clastic components are established, correlations between component abundances and rock density (as proxied by X-radiograph GSD) can be investigated. Because the GSD values of individual samples are influenced by multiple rock components that vary independently in abundance, it is necessary first to establish through multiple regression analysis that a particular set of components is responsible for a significant fraction of GSD variance. As organic carbon, Fe-sulfides, and phosphate are presumed to be the major components controlling GSD variation in the study units, sample GSD values were multiply regressed on TC, TS, and P_2O_5 concentrations. These three components collectively accounted for 71% of measured GSD variance in the Hushpuckney Shale, 87% in the Stark Shale, and 92% in the Muncie Creek Shale (Fig. 6). For individual study units, multiple regression r^2 values ranged from a low of 0.46 for the Ermal Hushpuckney to a high of 0.98 for the Heilman Stark (Table 1), demonstrating that organic carbon, Fe-sulfides, and phosphate were responsible for the majority of GSD variance in most study units. The significance of these correlations can be judged from F parameters (i.e., ratio of regression sum-of-squares to residual sum-of-squares) and significance levels $p(\alpha)$. All study units exhibit highly significant correlations ($F > 5$ and $p(\alpha) < 0.05$) between measured GSD values and the GSD values predicted on the basis of multiple regression analysis (Fig. 6) with the exception of the Edmonds Hushpuckney, which is marginally significant ($F = 4.7$, $p(\alpha) = 0.065$), and the Ermal Hushpuckney, which is non-significant ($F = 1.1$, $p(\alpha) = 0.433$; Table 1).

Assuming that a particular set of components accounts for a significant proportion of total GSD variance, it is necessary to establish whether all or only some of the components contribute to this relationship. The significance of the contributions of individual components to GSD variance can be determined through t tests of partial correlations between GSD values and TC, TS, and P_2O_5 concentrations; non-significant partial correlations ($p(\alpha) > .05$) are denoted by bracketed β -coefficients (i.e., multiple regression weights) for the relevant components in Table 1. Partial-correlation t tests revealed that (1) in five of eight study units (i.e., Edmonds Muncie Creek, Edmonds Stark, Womelsdorf Stark, Edmonds Hushpuckney, and Ermal Hushpuckney), TC was the only elemental parameter that significantly influenced GSD variance, (2) in the Ermal Stark and Heilman Stark, TC, TS, and P_2O_5 all contributed significantly to GSD variance, and (3) in the Mitchellson Hushpuckney only P_2O_5 did so (Table 1). Statistical checks for matrix ill-conditioning revealed no redundancy of components, and deletion of rare outliers identified through residuals analysis did not materially affect the results.

Once the major components that contribute significantly to GSD variance have been identified, GSD values can be used to predict the abundances of these components within portions of the study units that were not geochemically analyzed. Because this entails prediction of component abundances as a function of a single parameter (GSD), linear regression analysis is appropriate. First, it is necessary to establish that significant covariation exists between GSD and the elemental proxy for a given component in order for the former to have predictive value for the latter. Linear regression analysis revealed significant ($p(\alpha) < .05$) negative correlations between GSD and TC in seven out of eight study units, ranging from a low correlation coefficient (r) of -0.61 in the Ermal Hushpuckney to a high of -0.97 in the Womelsdorf Stark (Fig. 7); only the Mitchellson Hushpuckney yielded a non-significant GSD-TC correlation (Table 2). Thus, organic carbon concentrations can be reliably predicted from GSD values in most of the study units. In contrast, elemental proxies for the other major components (i.e., Fe-sulfides and phosphate) rarely exhibited significant covariance with GSD: (1) TS covaried positively with GSD in the Heilman Stark ($r = +0.61$; Fig. 8A), and (2) P_2O_5 covaried positively with GSD in the Mitchellson Hushpuckney ($r = +0.87$; Fig. 8B; Table 2). Thus, the ability to predict abundances of Fe-sulfides and phosphate in the study units from GSD values is severely limited.

Construction of Proxy Geochemical Records

The final step in the compositional analysis of black shales using X-radiograph GSD as a proxy for rock density entails transformation of the GSD record of the complete stratigraphic interval of interest to a proxy geochemical record, i.e., calculation of elemental concentrations in un-analyzed portions of study units on the basis of measured GSD values and GSD-elemental correlations. This procedure can be carried out for all elemental proxies whose concentrations exhibit a significant linear correlation with GSD (Table 2). Transformations of GSD values in the eight study units to TC, TS, and P_2O_5 concentrations are shown in Figures X and X of the companion paper.

Concentrations can be estimated for only a single elemental proxy in most study units. This reflects control of GSD values by a single dominant component in most units, i.e., by organic carbon in Edmonds Muncie Creek, Edmonds Stark, Ermal Stark, Womelsdorf Stark, Edmonds Hushpuckney, and Ermal Hushpuckney, and by phosphate in Mitchellson Hushpuckney (Table 2). The general dominance of organic carbon as a control on GSD values is due to the larger mean concentration and standard deviation of TC (18.7±8.2 wt%) relative to those of TS (2.13±0.69 wt%) and P_2O_5 (3.05±3.66 wt%; cf. Table 1). Rarely, concentrations for two or more elemental proxies may be estimated from the same GSD record, e.g., TC and TS in the Heilman Stark (Table 2).

Utility of X-radiography in Compositional Analysis

Because GSD-elemental correlations are dependent on lithologic peculiarities and operational considerations unique to a given study unit, such correlations must be established independently for each unit and cannot be inferred from analysis of other units (even of genetically related black shales, as in the present study). Different shales may exhibit substantially different compositional controls on GSD variance. For example, analysis of the Upper Devonian Cleveland Member of the Ohio Shale revealed that (1) for the formation as a whole, organic carbon and Fe-sulfides exerted subequal control on GSD values (accounting for 62% and 63% of total GSD variance, respectively), (2) the relative dominance of these components varied from cycle to cycle in the stratigraphic and

geographic dimensions, with the contribution to GSD variance of TC ranging from <10% to 85% and that of TS from <10% to 86%, and (3) phosphate exerted no control on GSD values (Jaminski et al. 1997). Differences in the dominant compositional controls on GSD variance in Ohio Devonian versus Midcontinent Pennsylvanian black shales reflect lower TC concentrations (mean $8.6 \pm 3.3\%$), higher and more variable TS concentrations (mean $2.90 \pm 1.63\%$), and a near-absence of P_2O_5 (<xx ppm, i.e., below detection limits) in the former relative to the latter.

In terms of efficiency of analysis, the utility of this technique depends on the stratigraphic thickness of the section of interest, dominant length scales of compositional variation, and the degree of variability in compositional patterns within the study unit. In the present study, in which geochemical analysis was undertaken on an average of 14 cm of each 50-cm-thick shale unit (i.e., 30% of total thickness), the efficiency gain was modest. However, application of the same set of procedures to the 20-m-thick Upper Devonian Cleveland Member of the Ohio Shale resulted in a considerable gain in efficiency, i.e., geochemical analysis of three 12-14-cm-thick intervals (representing ca. 2% of total unit thickness) was sufficient to characterize compositional variation and establish GSD-elemental proxy correlations in the study units (Jaminski et al. 1997).

CONCLUSIONS

Use of X-radiograph gray-scale density (GSD) as a proxy for rock density has considerable potential for generation of long, high-resolution paleoclimate proxy records in laminated organic-rich strata. Because variation in rock density in black shales is primarily controlled by a small number of non-clastic components (e.g., organic carbon, Fe-sulfide, and phosphate), correlation of elemental proxies for these components (e.g., TC, TS, and P_2O_5 , respectively) to GSD values can determine (1) which components contribute significantly to GSD variance, and (2) for which components GSD values can be used predictively, i.e., to estimate component abundance in un-analyzed portions of a study unit. This procedure permits rapid (ca. 30 cm hr^{-1}) analysis of fine-(sub-mm-) scale compositional variation in black shales and is largely non-destructive.

ACKNOWLEDGMENTS

We wish to thank Mark Thompson (Kentucky Geological Survey), Lisa Trump (University of Cincinnati) for drafting services, and Phil Heckel (University of Iowa) for helpful discussions and manuscript reviews. The study cores were kindly provided by the Kansas Geological Survey (KGS series).

REFERENCES

- ALGEO, T.J., AND WOODS, A.D., 1994, Microstratigraphy of the Lower Mississippian Sunbury Shale: A record of solar-modulated climatic cyclicity: *Geology*, v. 22, p. 795-798.
- ALGEO, T.J., PHILLIPS, M., JAMINSKI, J., AND FENWICK, M., 1994, High-resolution X-radiography of laminated sediment cores: *Journal of Sedimentary Research*, v. A64, p. 665-668.
- APLIN, A.C., BISHOP, A.N., CLAYTON, C.J., KEARSLEY, A.T., MOSSMANN, J.-R., PATIENCE, R.L., REES, A.W.G., AND ROWLAND, S.J., 1992, A lamina-scale geochemical and sedimentological study of sediments from the Peru Margin (Site 680, ODP Leg 112), in C.P. Summerhayes, W.L. Prell, and K.C.

- Emeis (Editors), *Upwelling Systems: Evolution Since the Early Miocene*: Geol. Soc. London Spec. Publ. 64, p. 131-149.
- BERNER, R.A., AND RAISWELL, R., 1983, Burial of organic carbon and pyrite sulfur in sediments over Phanerozoic time: A new theory: *Geochim. Cosmochim. Acta*, v. 47, p. 855-862.
- CANFIELD, D.E., RAISWELL, R., WESTRICH, J.T., REAVES, C.M., AND BERNER, R.A., 1986, The use of chromium reduction in the analysis of reduced inorganic sulfur in sediments and shales: *Chemical Geology*, v. 54, p. 149-155.
- COVENEY, R.M., JR., 1985, Temporal and spatial variations in Pennsylvanian black shale geochemistry, *in* W.L. Watney, R.L. Kaesler, and K.D. Newell (Editors), *Recent Interpretations of Late Paleozoic Cyclothems*: Kansas Geol. Surv., Lawrence, Kansas, p. 247-266.
- COVENEY, R.M., JR., LEVENTHAL, J.S., GLASCOCK, M.D., AND HATCH, J.R., 1987, Origins of metals and organic matter in the Mecca Quarry Shale Member and stratigraphically equivalent beds across the Midwest: *Economic Geology*, v. 82, p. 915-933.
- COVENEY, R.M., JR., AND SHAFFER, N.R., 1988, Sulfur-isotope variations in Pennsylvanian shales of the midwestern United States: *Geology*, v. 16, p. 18-21.
- COVENEY, R.M., JR., WATNEY, W.L., AND MAPLES, C.G., 1989, Rates and durations for the accumulation of Pennsylvanian black shales in the midwestern United States: Kansas Geological Survey, *Subsurface Geology Series 12*, p. 73-76.
- CROWELL, J.C., 1978, Gondwanan glaciation, cyclothems, continental positioning, and climate change: *American Journal of Science*, v. 278, p. 1345-1372.
- DESBOROUGH, G.A., HATCH, J.R., AND LEVENTHAL, J.S., 1991, Geochemical and mineralogical comparison of the Upper Pennsylvanian Stark Shale Member of the Dennis Limestone, east-central Kansas, with the Middle Pennsylvanian Mecca Quarry Shale Member of the Carbondale Formation in Illinois and of the Linton Formation in Indiana: U.S. Geological Survey Circular 1058, p. 12-30.
- HATCH, J.R., AND LEVENTHAL, J.S., 1992, Relationship between inferred redox potential of the depositional environment and geochemistry of the Upper Pennsylvanian (Missourian) Stark Shale Member of the Dennis Limestone, Wabaunsee County, Kansas, U.S.A.: *Chemical Geology*, v. 99, p. 65-82.
- HAY, B.J., HONJO, S., KEMPE, S., ITTEKKOT, V.A., DEGENS, E.T., KONUK, T., AND IZDAR, E., 1990, Interannual variability in particle flux in the southwestern Black Sea: *Deep-Sea Research*, v. 37, p. 911-928.
- HECKEL, P.H., 1977, Origin of phosphatic black shale facies in Pennsylvanian cyclothems of mid-continent North America: *American Association of Petroleum Geologists Bulletin*, v. 61, p. 1045-1068.
- HECKEL, P.H., 1984, Factors in Mid-Continent Pennsylvanian limestone deposition, *in* N.J. Hyne (Editor), *Limestones of the Mid-continent*, Tulsa Geol. Soc., Tulsa, Oklahoma, Spec. Publ. 2, p. 25-50.
- HECKEL, P.H., 1991, Thin widespread Pennsylvanian black shales of Midcontinent North America: A record of a cyclic succession of widespread pycnoclines in a fluctuating epeiric sea, *in* Tyson, R.V., and Pearson, T.H., eds., *Modern and Ancient Continental Shelf Anoxia*: Geological Society of London Special Publication 58, p. 259-273.
- HECKEL, P.H., 1994, Evaluation of evidence for glacial-eustatic control over marine Pennsylvanian cyclothems in North America and consideration of possible tectonic effects, *in* Dennison, J.M., and Ettensohn, F.R., eds., *Tectonic and Eustatic Controls on Sedimentary Cycles*: SEPM (Society for Sedimentary Geology), *Concepts in Sedimentology and Paleontology 4*, p. 65-87.
- HERBERT, T.D., AND FISCHER, A.G., 1986, Milankovitch climatic origin of mid-Cretaceous black shale

rhythms in central Italy: *Nature*, v. 321, p. 739-743.

- HERBERT, T.D., AND MAYER, L.A., 1991, Long climatic time series from sediment physical property measurements: *Journal of Sedimentary Petrology*, v. 61, p. 1089-1108.
- HOFFMAN, D.L., ALGEO, T.J., MAYNARD, J.B., JOACHIMSKI, M.M., HOWER, J.C., AND JAMINSKI, J., 1997, Microstratigraphic analysis of compositional variation in black shales: Offshore core shales in Upper Pennsylvanian cyclothems of the eastern Midcontinent Shelf (Kansas), USA, *in* Schieber, J., ed., *Recent Progress in Shale Research*: Stuttgart, Schweizerbart'sche.
- HUTTON, A.C., 1987, Petrographic classification of oil shales: *International Journal of Coal Geology*, v. 8, p. 203-231.
- JAMINSKI, J., ALGEO, T.J., MAYNARD, J.B., AND HOWER, J.C., 1997, Microstratigraphic analysis of compositional variation in black shales: The Cleveland Member of the Ohio Shale (Upper Devonian), central Appalachian Basin, USA, *in* Schieber, J., ed., *Recent Progress in Shale Research*: Stuttgart, Schweizerbart'sche.
- JARVIS, I., BURNETT, W.C., NATHAN, Y., and 9 others, 1994, Phosphorite geochemistry: State-of-the-art and environmental concerns: *Eclog. geol. Helv.*, v. 87, p. 643-700.
- KOCH, G.S., JR., AND LINK, R.F., 1971, *Statistical Analysis of Geological Data*, v. 2: Dover, New York, 438 p.
- LYONS, T.W., 1991, Upper Holocene sediments of the Black Sea: Summary of Leg 4 box cores (1988 Black Sea Oceanographic Expedition), *in* Izdar, E., and Murray, J.W., eds., *Black Sea Oceanography*: Kluwer, Dordrecht, p. 401-441.
- MAYER, L.A., JANSEN, E., BACKMAN, J., AND TAKAYAMA, T., 1993, Climatic cyclicality at Site 806: The GRAPE record, *in* Berger, W.H., Kroenke, L.W., Mayer, L.A., et al., eds., *Proceedings of the Ocean Drilling Program: Scientific Results*, v. 130, p. 623-639.
- MCKINSEY, T.R., AND KEPFERLE, R.C., 1985, X-radiography of the New Albany and Chattanooga Shales (Devonian) along the western flank of the Cincinnati Arch in Kentucky, *in* *Proceedings of the 1985 Eastern Oil Shale Symposium*, Institute for Mining and Minerals Research, Lexington, Kentucky, p. 261-267.
- PETERSON, L.C., OVERPECK, J.T., KIPP, N.G., AND IMBRIE, J., 1991, A high-resolution Late Quaternary upwelling record from the anoxic Cariaco Basin, Venezuela: *Paleoceanography*, v. 6, p. 99-119.
- POTTER, P.E., MAYNARD, J.B., AND PRYOR, W.A., 1982, Appalachian gas-bearing Devonian shales: Statements and discussion: *Oil and Gas Journal*, v. 80, p. 290-316.
- REPETA, D.J., 1993, A high resolution historical record of Holocene anoxygenic primary production in the Black Sea: *Geochimica et Cosmochimica Acta*, v. 57, p. 4337-4342.
- RIPEPE, M., ROBERTS, L.T., AND FISCHER, A.G., 1991, ENSO and sunspot cycles in varved Eocene oil shales from image analysis: *Journal of Sedimentary Petrology*, v. 61, p. 1155-1163.
- ROBL, T.L., BLAND, A.E., KOPPENAAL, D.W., AND BARRON, L.S., 1983, Geochemistry of oil shales in eastern Kentucky, *in* F.P. Miknis, and J.F. McKay, J.F. (Editors), *Geochemistry and Chemistry of Oil Shale*: American Chemical Society, Washington, D.C., p. 159-180.
- SAGEMAN, B.B., RICH, J., ARTHUR, M.A., BIRCHFIELD, G.E., AND DEAN, W.E., 1997, Evidence for Milankovitch periodicities in Cenomanian-Turonian lithologic and geochemical cycles, western interior U.S.A.: *Journal of Sedimentary Research*, v. 67, p. 286-302.
- SCHULTZ, R.B., AND COVENEY, R.M., JR. (1992): Time-dependent changes for Midcontinent Pennsylvanian

black shales: *Chemical Geology*, v. 99, p. 83-100.

TYSON, R.V., 1995, *Sedimentary Organic Matter*: Chapman & Hall, London, 615 pp.

VEEVERS, J.J., AND POWELL, C.M., 1987, Late Paleozoic glacial episodes in Gondwanaland reflected in transgressive-regressive depositional sequences in Euramerica: *Geological Society of America Bulletin*, v. 98, p. 475-487.

WATNEY, W.L., 1980, Cyclic sedimentation of the Lansing-Kansas Groups in northwestern Kansas and southwestern Nebraska: *Kansas Geological Survey Bulletin* 220, 72 p.

WATNEY, W.L., FRENCH, J.A., AND FRANSEEN, E.K., 1989, Sequence stratigraphic interpretations and modeling of cyclothems in the Upper Pennsylvanian (Missourian) Lansing, and Kansas City groups in eastern Kansas: *Kansas Geol. Soc., Lawrence, Kansas, 41st Annual Fieldtrip Guidebook*, 211 pp.

WATNEY, W.L., FRENCH, J.A., DOVETON, J.H., YOULE, J.C., AND GUY, W.J., 1995, Cycle hierarchy and genetic stratigraphy of Middle and Upper Pennsylvanian strata in the upper Mid-continent, *in* Hyne, N.J., ed., *Sequence Stratigraphy of the Mid-Continent*: Tulsa, Oklahoma, Tulsa Geological Society Special Publication 4, p. 141-192.

WENGER, L.M., AND BAKER, D.R., 1986, Variations in organic geochemistry of anoxic-oxic black shale-carbonate sequences in the Pennsylvanian of the Midcontinent, U.S.A.: *Organic Geochemistry*, v. 10, p. 85-92.

TABLE 1. MULTIPLE REGRESSION STATISTICS

Core	TC*	TS*	P ₂ O ₅ *	r ²	n	F [†]	p(α)	β ₀ [§]	β ₁ [§]	β ₂ [§]	β ₃ [§]
<u>MUNCIE CREEK</u>											
Edmonds	20.6±9.9	1.33±0.18	1.11±2.55	0.92	9	20.5	0.003	331.6	-7.86	(1.60)	(-22.5)
<u>STARK</u>											
Edmonds	22.2±8.4	3.09±0.72	0.86±1.85	0.86	12	14.2	0.002	409.6	-8.89	(-18.0)	(-0.143)
Ernal	19.8±5.6	2.53±0.61	2.06±2.51	0.96	13	78.0	0.000	143.0	-10.10	63.0	17.23
Womelsdorf	19.4±7.0	2.47±0.20	1.87±2.67	0.96	13	21.4	0.016	228.7	-7.64	(23.7)	(-4.25)
Heilman	16.9±4.6	1.93±0.43	4.10±2.70	0.98	13	123.5	0.000	190.6	-12.82	55.1	15.13
<u>HUSHPUCKNEY</u>											
Edmonds	26.4±5.5	2.12±0.43	6.51±4.78	0.74	9	4.7	0.065	117.9	-5.10	(3.72)	(31.1)
Ernal	28.8±5.8	2.58±0.67	4.36±4.47	0.46	14	1.1	0.433	164.5	-7.82	(1.66)	(51.8)
Mitchellson	15.1±3.4	1.64±0.40	3.61±4.70	0.84	10	10.3	0.009	22.9	(0.30)	8.81	(47.1)

*Mean component concentrations in weight percent.

[†]F = SS_{regression}/SS_{residual}.

[§]Regression weights: β₀ (Y-intercept), β₁ (TC), β₂ (TS), β₃ (P₂O₅); non-significant beta coefficients (p(α) > 0.05) based on t tests of partial correlations given in parentheses.

TABLE 2. LINEAR REGRESSION STATISTICS

Core		Predicted Concentration*	Std. Err. (Y)	r†
<u>MUNCIE CREEK</u>				
Edmonds	TC	37.10-0.1166 γ	3.11	-0.96
<u>STARK</u>				
Edmonds	TC	37.80-0.0996 γ	3.76	-0.92
Ermal	TC	32.33-0.0870 γ	4.22	-0.75
Ermal	TS	3.208-0.00466 γ	0.62	(-0.36)
Ermal	P ₂ O ₅	0.255+0.0125 γ	2.65	(0.23)
Womelsdorf	TC	36.34-0.130 γ	2.36	-0.97
Heilman	TC	24.24-0.0512 γ	3.74	-0.73
Heilman	TS	1.296+0.00440 γ	0.37	0.61
Heilman	P ₂ O ₅	3.250+0.00597 γ	2.91	(0.13)
<u>HUSHPUCKNEY</u>				
Edmonds	TC	32.30-0.0805 γ	4.94	-0.62
Ermal	TC	30.57-0.0726 γ	8.52	-0.61
Mitchellson	P ₂ O ₅	-5.829+0.0690 γ	2.55	0.87

*Concentrations in weight percent; γ = gray-scale density.
†Non-significant correlation coefficients in parentheses.

FIGURE CAPTIONS

FIG. 1.--Flow chart of procedure for X-radiography-based analysis of compositional variation in black shales.

FIG. 2.--Dm-scale compositional cyclicity in Upper Pennsylvanian Midcontinent offshore black shales. The example shown is from the Stark Shale in the Edmonds core; geochemical and petrographic data were generated only for a 16-cm-thick interval (out of a total thickness of 60 cm), and compositional variation in the remainder of the study unit was reconstructed based on GSD-elemental proxy correlations (see companion paper).

FIG. 3.--Carbonate content of a representative subset of samples from the study units ($n = 17$), based on carbonate bomb analysis in which CO_2 was evolved via acidization of a powdered sample. A regression line and 95% confidence band (Koch and Link 1971) were calculated for pure CaCO_3 standards (circles). Carbonate percentages were calculated using a fractional CaCO_3 scale (expanded view on right) and have uncertainties of $\pm 16\%$ of the estimated value (i.e., width of the regression confidence band). Weights of standards (0.1-0.5 g) are smaller than those of samples (ca. 2 g) owing to the limited volumetric capacity of the carbonate bomb (<100 ml evolved CO_2). Total inorganic carbon (TIC) concentration is related to percent carbonate (CaCO_3) by a factor of 0.12 (i.e., 12 g C 100 g⁻¹ CaCO_3). Because the tested samples yielded uniformly low TIC values (mean $0.9 \pm 0.9\%$ and max. 2.6% of total carbon), it was deemed unnecessary to determine inorganic C concentrations for the full sample set.

FIG. 4.--Sulfur-iron relations for all samples from the study units ($n = 85$). Fe values are given as elemental rather than oxide concentrations; stoichiometric pyrite corresponds to a 2:1 S:Fe ratio (solid line), and S:Fe ratios of 1.5:1 and 1:1 are shown as dotted lines. Note that, although most samples contain "excess" Fe, S-Fe covariation is generally positive and strongly so for the Edmonds Stark and Ermal Stark shales (dashed fields). Symbols: Hushpuckney Shale circles (Edmonds core = filled; Ermal core = half-filled; Mitchellson core = dotted); Stark Shale squares (Edmonds core = filled; Ermal core = half-filled; Womelsdorf core = dotted; Heilman core = open); Muncie Creek Shale triangles (Edmonds core = filled); the same symbols are used for identification of individual study units in subsequent figures.

FIG. 5.--Calcium-phosphorus relations for all samples from the study units ($n = 85$); symbols as in Figure 4. Strong covariation between CaO and P_2O_5 ($r^2 = 0.95$; $p(\alpha) < 0.001$) indicates that both elements reside mainly in authigenic phosphate. A positive X-intercept (3.8 wt% CaO) suggests that a small and relatively constant amount of calcium is present in non-phosphatic phases (e.g., clay minerals). A slope of 0.48 for the CaO- P_2O_5 regression (solid line) is less than the expected slope of 0.76 (dashed line) for stoichiometric francolite (calcium fluorapatite, or $\text{Ca}_5(\text{PO}_4)_3\text{F}$), implying that phosphate nodules in the study units have a uniformly P-poor composition.

FIG. 6.--Measured gray-scale density vs. predicted gray-scale density for the Muncie Creek (A), Stark (B), and Hushpuckney shales (C; $n = 80$); symbols as in Figure 4. Predicted GSD values are based on multiple regression of GSD on the concentrations of TC, TS, and P_2O_5 , which are elemental proxies for organic carbon, Fe-sulfide, and phosphate, respectively. Strong positive covariance of measured and predicted GSD values ($r^2 = 0.71-0.92$) indicates that these three rock components account for the majority of GSD variance in the study units.

FIG. 7.--Gray-scale density versus total carbon for the Muncie Creek (A), Stark (B-C), and Hushpuckney shales (D); symbols as in Figure 4. Correlation correlations (r ; Table 2) are significant at $p(\alpha) < 0.01$ for all Muncie Creek and Stark units and at $p(\alpha) < 0.05$ for Hushpuckney units other than the Mitchellson core (dotted line, D). In the Mitchellson Hushpuckney, GSD is not significantly related to TC, and the dominant control on GSD variance is P_2O_5 (see Fig. 8B).

FIG. 8.--Gray-scale density versus TS for the Heilman Stark (A), and gray-scale density versus P_2O_5 for the Mitchellson Hushpuckney (B). The correlation coefficients for A ($r = +0.87$) and B ($r = +0.61$) are significant at $p(\alpha) < 0.01$ and < 0.05 , respectively (Table 2).

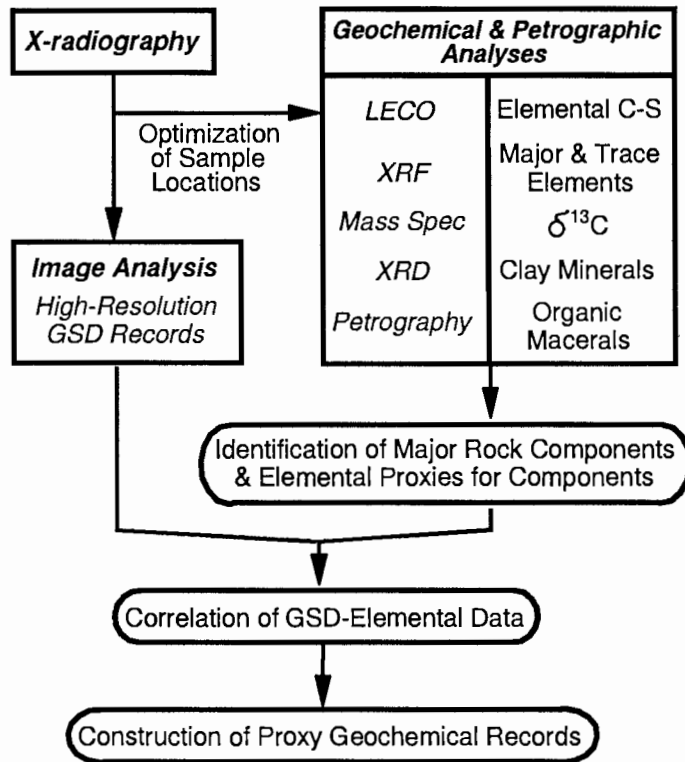


FIGURE 1

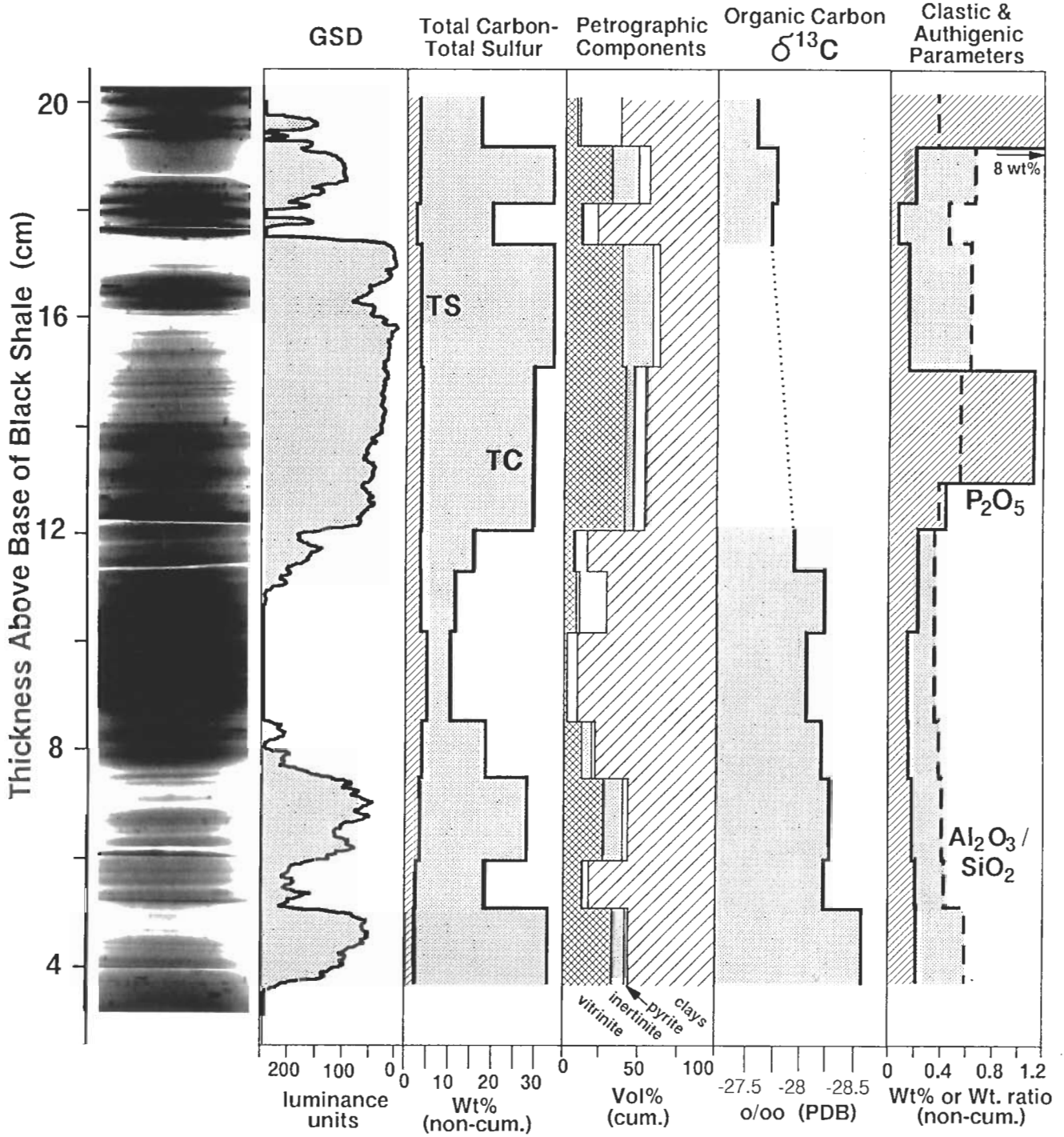


FIGURE 2

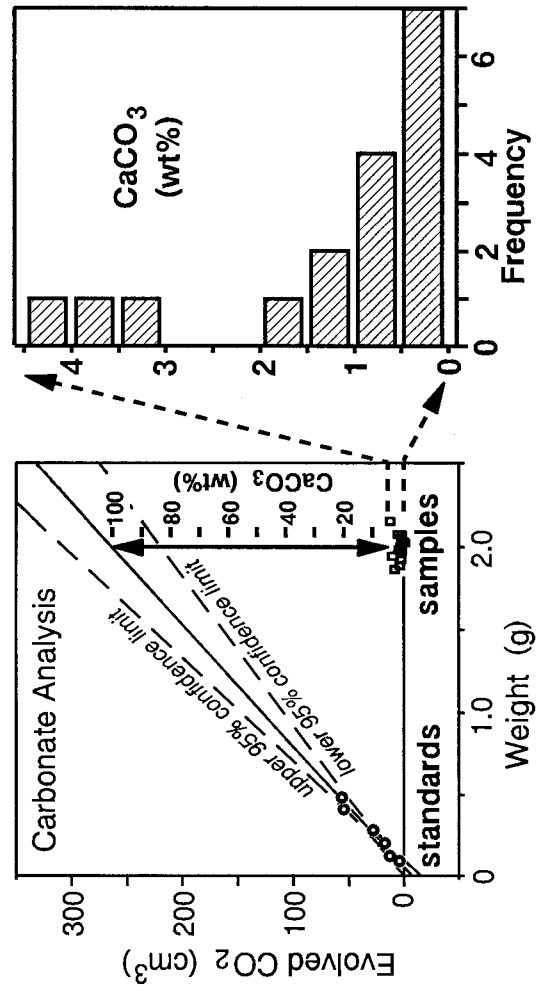


FIGURE 3

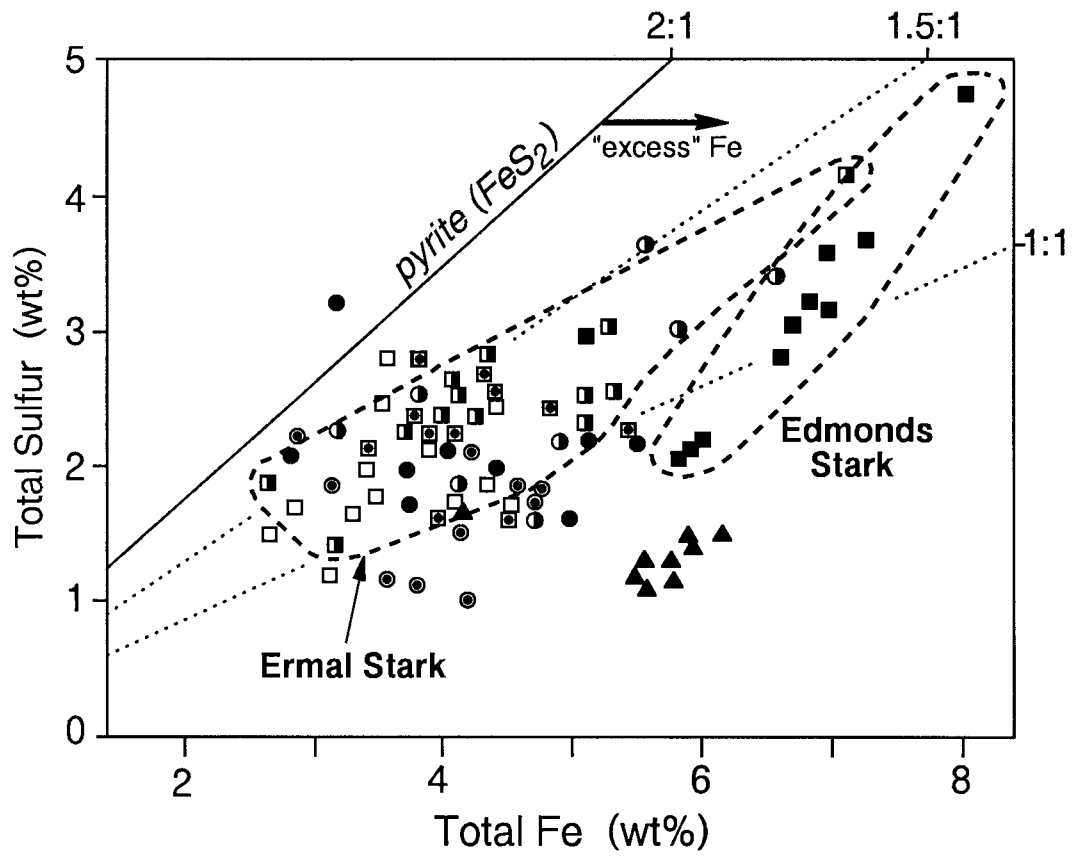


FIGURE 4

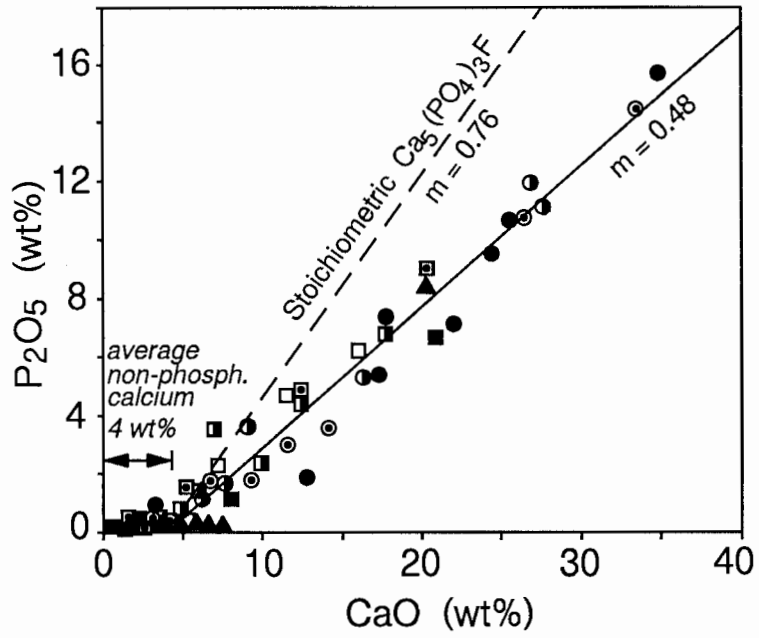


FIGURE 5

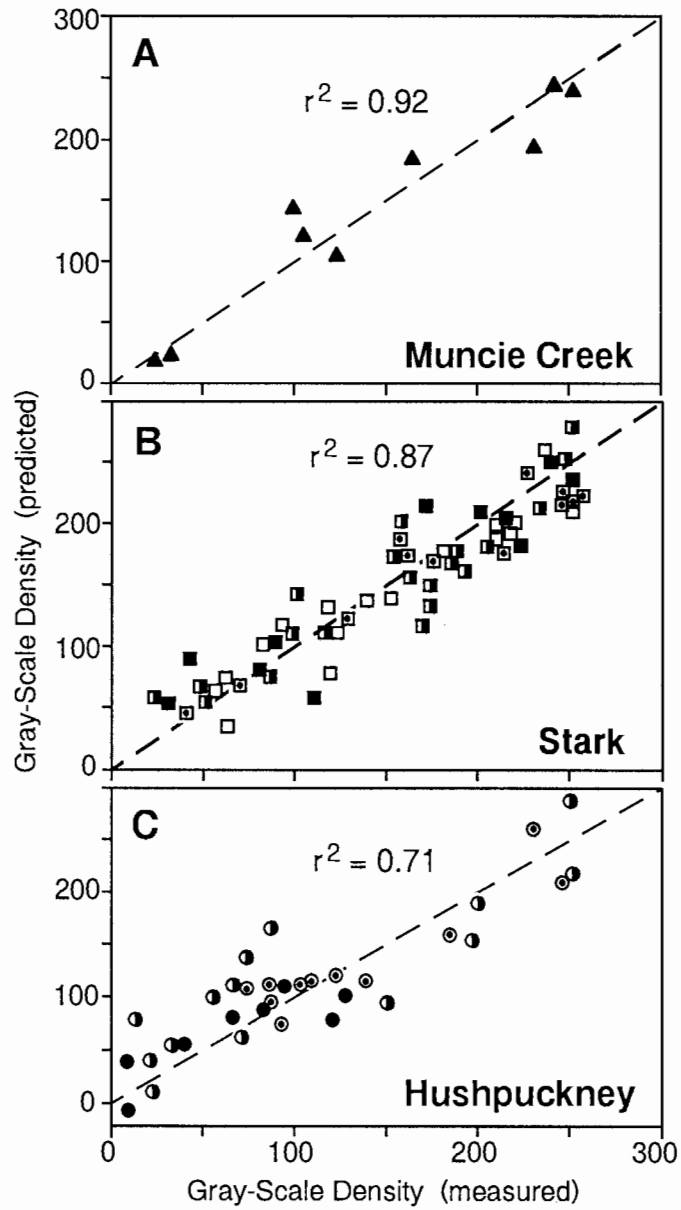


FIGURE 6

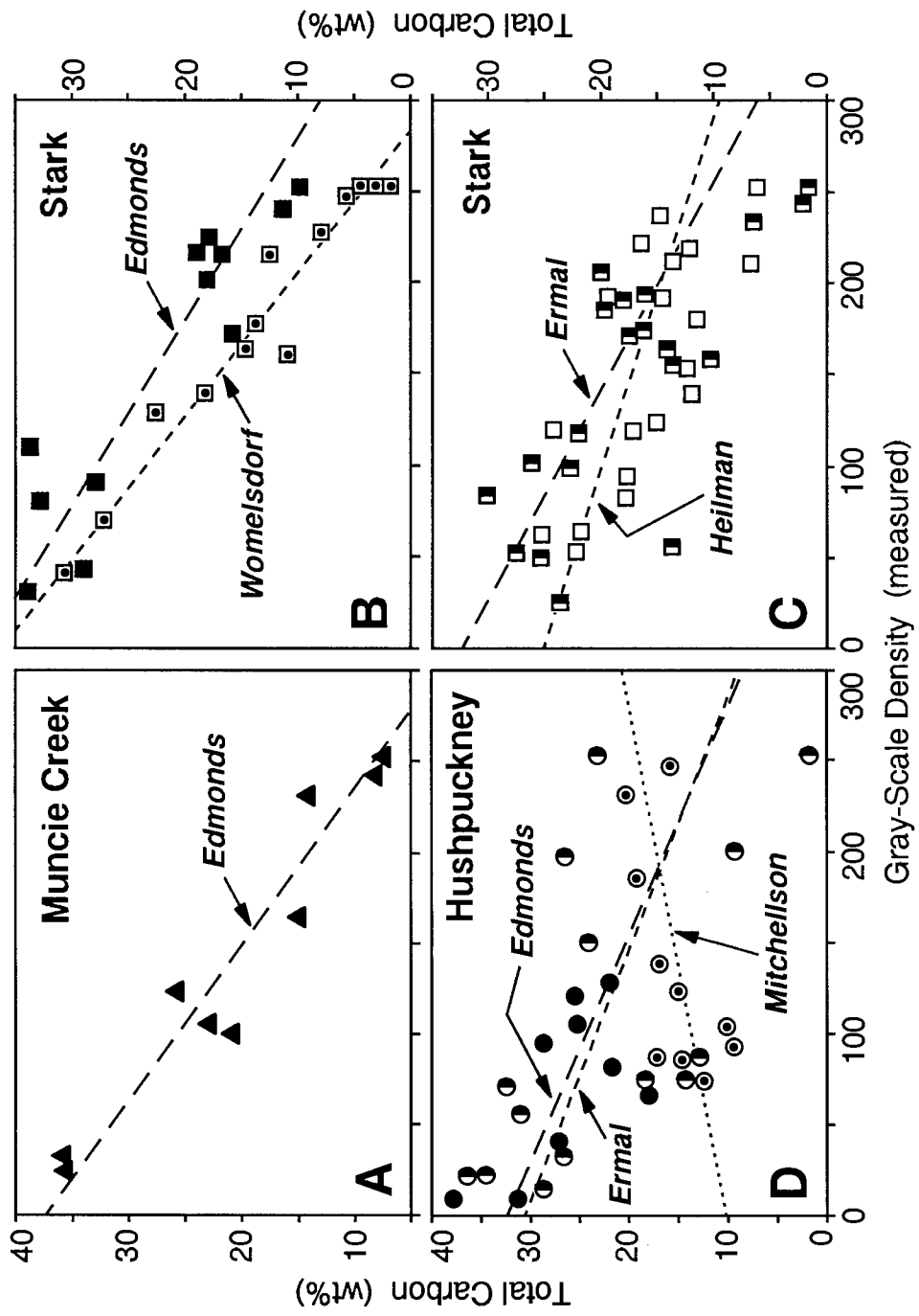


FIGURE 7

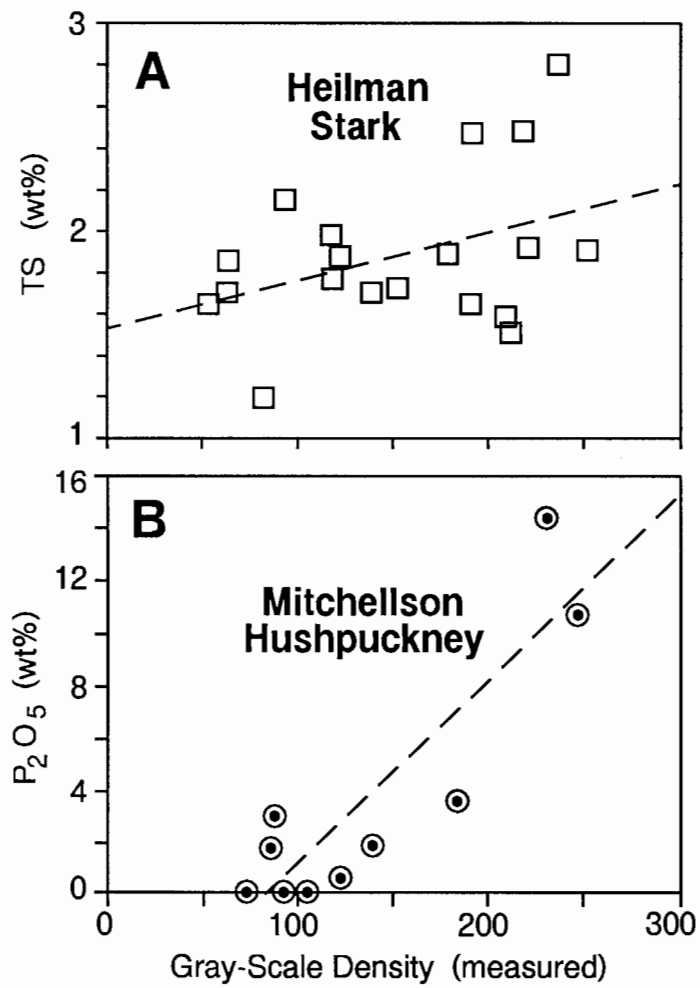


FIGURE 8